Joint Trajectory Optimization for Multiple Automated Vehicles in Lane-free Traffic with Vehicle Nudging*

Niloufar Dabestani, Panagiotis Typaldos, Venkata K. Yanumula, Ioannis Papamichail and Markos Papageorgiou, *Life Fellow*, *IEEE*

***Abstract*— This paper presents a joint trajectory optimization algorithm for a number of connected and automated vehicles in a lane-free traffic environment with vehicle nudging. A double-integrator model is assumed for the longitudinal and lateral movement of each one of the vehicles, considering constant and state-dependent bounds on control inputs, including road boundary constraints. A multi-objective function is designed for all vehicles and is minimized using an efficient feasible direction algorithm. This leads to minimization of fuel consumption, collision avoidance, achievement of desired speeds and prevention of infeasible maneuvers. Challenging scenarios are examined on a lane-free straight motorway stretch, producing promising results for further exploration in situations where simultaneous trajectory optimization for groups of vehicles (e.g., vehicle flocks or two-dimensional platoons) is considered.**

***Index terms*— Lane-free traffic, automated vehicles, joint path planning, optimal coordination, trajectory planning.**

I. Introduction

Over the past few decades, there has been a significant endeavor by both the automotive industry and research institutions to plan, develop, test and deploy a variety of vehicle automation and communication technologies. These innovations are expected to fundamentally transform the functions and abilities of individual vehicles [1]. Connected automated vehicles (CAVs) gather information from their own sensors, from other vehicles and from the road infrastructure to improve their performance and safety; and have the potential to contribute to mitigating many persisting issues, such as traffic congestion, inefficient fuel consumption and road accidents [2]. To achieve these goals, vehicle-to-vehicle (V2V) and vehicle-to-infrastructure (V2I) communication systems, collectively known as V2X, are being developed to facilitate the corresponding communication channels [3].

In this context, the *TrafficFluid* concept was recently introduced, as a novel paradigm for vehicular traffic in the era of CAVs which is expected to prevail in the not-too-far future. *TrafficFluid* envisions CAVs driving according to the following two combined principles [4]: (i) Lane-free movement on the 2-D road surface, meaning that vehicles are not bounded in traffic lanes; (ii) Vehicle nudging, i.e. vehicles may be influencing (via sensors or communication) other vehicles in front of them.

Many works proposed algorithms for CAV driving based on various methodological avenues, see [5, 6] for related reviews. One such avenue, involving several approaches and methods, is the use of optimization and optimal control to derive CAV trajectories under diverse settings, see [7] for a review. These works address lane-based CAV driving; therefore, they mostly focus on the longitudinal motion; while, in some works, lateral motion in the form of lane-changing decisions is also included, see e.g. [8, 9, 10].

While the vast majority of proposed CAV driving methods address one vehicle at a time, an interesting question refers to possible performance gains achievable if multiple vehicle trajectories would be optimized jointly. This is indeed considered in research addressing signal-free urban junction crossing or automated highway merging [11] but is less common for highway driving vehicles. More specifically, works on the subject of optimal 2-D joint trajectory planning for multiple vehicles in lane-based traffic is limited, because lateral vehicle positions are discrete (on lanes), not real-valued, except for special circumstances, such as during lane changing. Solution of discrete optimization problems is computationally expensive even for a single vehicle. In [12], a trajectory planning model is proposed for lane-changing, involving multiple vehicles, using optimal control. The method first selects small vehicle groups that are deemed worthy of being jointly optimized and supports mandatory lane changes only, not optional lane changes. A mixed-integer-quadratic-programming problem for multiple automated vehicles is formulated in [13] to minimize a collective cost function. However, due to the presence of integer variables, the method does not scale well, hence joint optimization may be limited to very few vehicles at a time. In [14], an optimization problem is solved for groups of CAVs on lane-based freeways to benefit fuel consumption, desired speed driving and safe lane-changing, whereby collision avoidance is imposed via a nonlinear constraint. The number of vehicles in each group and the optimization time horizon are kept small due to computational complexity, and the method is mainly aimed at facilitating lane changes, in particular at difficult traffic infrastructures, such as in weaving sections. A genuinely lane-free approach is proposed in [15], where nonlinear model predictive control is adopted for cooperative path planning of multiple autonomous vehicles. The controller is tested on a curvy road for a large group of vehicles and

*The research leading to these results has received funding from the European Research Council under the European Union's Horizon 2020 Programme / ERC Grant Agreement no. 833915, project TrafficFluid, see: https://www.trafficfluid.tuc.gr

All the authors are with Dynamic Systems and Simulation Laboratory, Technical University of Crete, Chania, Crete, 73100, Greece.

e-mails: {ndabestani, ptypaldos, karteek, ipapa, markos}@dssl.tuc.gr

Markos Papageorgiou is also with the Faculty of Maritime and Transportation, Ningbo University, Ningbo, China.

compares their traffic flow and objective function value in a lane-based versus lane-free environment. It should be noted that the required computation times are not detailed in [12-15] to enable a more accurate assessment of the involved computational effort.

Other works in the area of robotics [16] and unmanned aerial vehicles (UAVs) consider centralized trajectory planning problems, which resemble vehicle trajectory planning problems on a lane-free road. In [17] a review is provided that addresses different optimization methods, such as particle swarm [18] or ant colony [19], applied to UAVs to improve their cooperative motion planning. However, bio-inspired optimization methods can be slow to find the optimal solution.

In [20], a single-vehicle nonlinear constrained optimal control problem is formulated and solved numerically through a Feasible Direction Algorithm (FDA) in a Model Predictive Control (MPC) framework with finite time horizons of 8 s. The MPC is applied independently to every individual CAV driving on a lane-free ring-road where vehicles may be nudging each other. An interesting topic, also in this lane-free context, is joint trajectory specification for a (big or small) group of vehicles. This is particularly appealing in lane-free driving where all involved variables are real-valued, and FDA is known to exhibit polynomial complexity. As a first step in this direction, this article generalizes the formulation of [20] to form a centralized nonlinear constrained Optimal Control Problem (OCP), with both fixed and state-dependent bounds on control inputs, for joint trajectory planning for a number of CAVs, in a lane-free traffic environment with vehicle nudging. The OCP is solved numerically via the efficient FDA and is applied simultaneously to all involved vehicles. It is demonstrated that the approach can be applied to dozens of vehicles simultaneously considering long simulation time horizons, since the proposed algorithm is very efficient.

The rest of the paper is organized as follows: Section II-A describes the problem variables, state equations and constraints. Section II-B presents the multi-objective function considered. Section III outlines the numerical solution algorithm, while Section IV presents two collective driving scenarios considered and the corresponding results. Finally, Section V addresses concluding remarks and points to some of the on-going and future work.

II. OPTIMAL CONTROL PROBLEM (OCP)

In this section a discrete-time OCP is formulated for a number of vehicles. State equations, constraints and an objective function, whose minimization provides jointly optimal trajectories for all the vehicles, are described.

A. Problem Variables, State Equations and Constraints

Assuming a number of vehicles, the movement of each vehicle i is defined by four state equations (see also [20]):

$$\begin{aligned} x_i(k+1) &= x_i(k) + Tv_{x,i}(k) + \tfrac{1}{2}T^2 a_{x,i}(k) \\ y_i(k+1) &= y_i(k) + Tv_{y,i}(k) + \tfrac{1}{2}T^2 a_{y,i}(k) \\ v_{x,i}(k+1) &= v_{x,i}(k) + Ta_{x,i}(k) \\ v_{y,i}(k+1) &= v_{y,i}(k) + Ta_{y,i}(k) \end{aligned} \tag{1}$$

where x_i and y_i are longitudinal and lateral positions, respectively; $v_{x,i}$ and $v_{y,i}$ are longitudinal and lateral speeds; $a_{x,i}$ and $a_{y,i}$ are control inputs reflecting the longitudinal and lateral accelerations; k is the discrete time integer index and T is the step size, related to time t via $t = kT$.

Longitudinal and lateral accelerations are bounded (see also [20]):

$$\begin{aligned} a_{x,i}^{\min}(\boldsymbol{x}(k),k) \le a_{x,i}(k) \le a_{x,i}^{\max}(k) \\ a_{y,i}^{\min}(\boldsymbol{x}(k),k) \le a_{y,i}(k) \le a_{y,i}^{\max}(\boldsymbol{x}(k),k) \end{aligned} \tag{2}$$

where $\boldsymbol{x}$ is the vector of all the states mentioned in (1). The upper bound of longitudinal acceleration is $a_{x,i}^{\max}(k) = A^{\max}$, where $A^{\max}$ is a constant and is chosen based on vehicle capabilities in accelerating. The lower limit of longitudinal acceleration is defined based on two requirements, namely non-negativity of longitudinal speed and a constant $A^{\min}$, reflecting vehicle's capability in decelerating, as follows:

$$a_{x,i}^{\min}(\boldsymbol{x}(k),k) = \max\{-\frac{1}{T}v_{x,i}(k), A^{\min}\} \tag{3}$$

The lateral acceleration bounds ensure that vehicles move within the road boundaries or exactly on a road boundary. In this study, the road boundaries are considered to be straight lines. As explained in [20], every vehicle located within the road boundaries at time steps k and $k+1$ should remain within the road boundaries at time step $k+2$ as well:

$$\tilde{y}_i \le y_i(k+2) \le \hat{y}_i \tag{4}$$

where $\hat{y}_i$ and $\tilde{y}_i$ are the lateral positions of the left and right road boundary, respectively. If the left or right constraint above is activated, meaning that the vehicle reaches left or right road boundary, then lateral speed $v_{y,i}$ must be zero, as otherwise the vehicle would exit the road. Replacing lateral position y_i and lateral speed $v_{y,i}$ from (1) in (4), yields, after some rearrangements, state-dependent bounds on lateral acceleration, which can be interpreted as dead-beat controllers that drive the vehicle towards the corresponding road boundary and its lateral speed to zero in two time-steps, as explained in [20]. Generalizing the dead-beat controller to allow for smoother and asymptotic boundary approach, we obtain the following state-dependent lateral control bounds:

$$\begin{aligned} a_{y,i}^{\min}(\boldsymbol{x}(k),k) = -K_{lat}\left[y_i(k) - \tilde{y}_i\right] \\ + (\frac{T}{2}K_{lat} - 2\sqrt{K_{lat}})v_{y,i}(k) \end{aligned} \tag{5}$$

$$\begin{aligned} a_{y,i}^{\max}(\boldsymbol{x}(k),k) = -K_{\text{lat}}\left[y_i(k) - \hat{y}_i\right] \\ + (\frac{T}{2}K_{\text{lat}} - 2\sqrt{K_{\text{lat}}})v_{y,i}(k) \end{aligned} \tag{6}$$

where $0 < K_{\text{lat}} \le 1/T^2$ is a feedback controller gain that may be tuned appropriately for smooth boundary approach, while asymptotic behavior is inherently guaranteed.

In this paper, state-dependent control bounds are transformed to constant control bounds by replacing the original control variables $a_{x,i}$ and $a_{y,i}$ with the following equations:

$$a_{x,i}(k) = (1-u_x(k))a_{x,i}^{\min}(\boldsymbol{x}(k),k) + u_x(k)a_{x,i}^{\max}(k)$$
$$a_{y,i}(k) = (1-u_y(k))a_{y,i}^{\min}(\boldsymbol{x}(k),k) + u_y(k)a_{y,i}^{\max}(\boldsymbol{x}(k),k) \quad (7)$$

Then, the new control variables u_x and u_y have constant bounds $0 \le u_x, u_y \le 1$.

B. Objective Function

A number of vehicles are taken into account, featuring pre-specified longitudinal and lateral desired speeds. The objective function consists of several sub-objectives in order to consider various goals, including passenger comfort, fuel consumption, reaching the desired speeds for all the vehicles, collision avoidance and mitigation of infeasible maneuvers. It should be noted that each sub-objective must be continuous and differentiable (see also [20]).

Fuel Consumption and Passenger Comfort: It is well known that high values or abrupt changes in longitudinal and lateral acceleration may affect fuel consumption and comfort of the passengers. Therefore, two quadratic cost terms of longitudinal and lateral accelerations, $a_{x,i}(k)^2$ and $a_{y,i}(k)^2$, are considered to be minimized for each vehicle i [20, 21].

Desired Speed: In this study, all vehicles are trying to reach their longitudinal and lateral desired speeds, $(v_{x,i}^*, v_{y,i}^*)$, in a coordinated way. For each vehicle i, two quadratic cost terms, $(v_{x,i}(k) - v_{x,i}^*)^2$ and $(v_{y,i}(k) - v_{y,i}^*)^2$, are used to penalize the deviations of longitudinal and lateral speeds from their respective desired values. $v_{x,i}^*$ is set to a positive value, while $v_{y,i}^*$ is set to zero to suppress unnecessary lateral movements.

Collision Avoidance: This sub-objective prevents each vehicle i from colliding with other vehicles. Intuitively speaking, if a vehicle i approaches a vehicle j (or vice-versa), vehicle i faces an ellipsoid around vehicle j, which reflects a cost. If vehicle i is positioned within the ellipsoid of vehicle j, the cost assumes a corresponding value. Since the problem solution tries to minimize the cost, it would repel vehicles i and j away from each other. The size of the cost ellipsoid depends on the positions and speeds of both vehicles. With l_i and l_j being the lengths of vehicles i and j, w_i and w_j being their widths, the length and width of the ellipsoid, if both vehicles are at stillstand, are computed as $L_i = 0.5\mu_x(l_i + l_j)$ and $W_i = 0.5\mu_y(w_i + w_j)$ where $\mu_x, \mu_y > 1$ are additional safety factors. If the vehicles are moving, the ellipsoid is augmented by use of time-gaps (ω_1, ω_2) in longitudinal and lateral directions of the cost ellipsoid to account for limited acceleration capabilities, see [20] for details. Note that the ellipsoid needs to have curvy longitudinal edges to allow faster vehicles behind to slide around and overtake slower vehicles. Considering also some more elaborated requirements that are detailed in [20], the ellipsoid cost function used to penalize vehicles approaching too close to each other is as follows:

$$c_{ij}(\boldsymbol{x}_i, \boldsymbol{x}_j) = \{1 - \tanh[(\frac{x_i - \delta_{x_j}}{0.5d_1})^{p_1} + (\frac{y_i - y_j}{0.5d_2})^{p_2}] + \frac{1}{[(\frac{x_i - \delta_{x_j}}{0.25d_1})^{p_3} + (\frac{y_i - y_j}{0.25d_2})^{p_4} + 1]^{p_5}}\} \quad (8)$$

where

$$\delta_{x_j} = x_j - (\omega_1(v_{x,i} - v_{x,j})/2) \quad (9)$$

d_1 and d_2 are given by

$$d_1 = L_i + \omega_1 v_{x,i} + \omega_1 v_{x,j}$$
$$d_2 = W_i + \omega_2[(\tanh(y_j - y_i))(v_{y,i} - v_{y,j}) + \sqrt{(\tanh(y_j - y_i))^2 (v_{y,i} - v_{y,j})^2 + \varepsilon_\omega}] \quad (10)$$

where ε_ω is a small positive value. Notice that this cost function is symmetric, i.e., we have $c_{ij} = c_{ji}$, and that it must apply to all vehicle couples. Thus, considering a group of n vehicles, the complete collision avoidance sub-objective is $\sum_{j=i+1}^{n} c_{ij}(\boldsymbol{x}_i, \boldsymbol{x}_j)$. Fig. 1 illustrates the collision avoidance function as seen by vehicle i, which is moving with $(v_x, v_y) = (30.0, 0.0)$m/s longitudinal and lateral speeds. Two vehicles positioned at $(x, y) = (30.0, 2.5)$m and $(x, y) = (40, 7.5)$m are moving with speeds $(v_x, v_y) = (25.0, 0.0)$m/s and $(v_x, v_y) = (35.0, 0.0)$m/s. In this example, the dimensions of all vehicles are identical with lengths of 4.25 m and widths of 1.8 m. Time-gaps (ω_1, ω_2) are (0.35,0.5) s, while (μ_x, μ_y) are (1.3,1.2), and exponents of the ellipsoid are $p_1 = 6$, $p_2 = p_3 = p_4 = p_5 = 2$. In Fig. 1, the blue rectangles represent the two encountered vehicles; therefore, if vehicle i is located at the position of the green rectangle, the value of collision avoidance cost is zero. Notice that, as the ellipsoid extends both upstream and downstream of the physical vehicle dimensions, upstream vehicles may influence downstream vehicles, i.e., vehicle nudging is incorporated in the collision avoidance term.

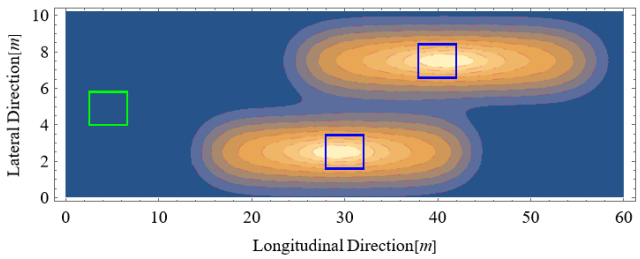

Figure 1. Illustration of collision avoidance function

Coupling of Longitudinal and Lateral Speeds: According to the vehicle dynamics in (1), longitudinal and lateral movements are decoupled, which is not deemed problematic if vehicles are moving at high longitudinal speeds. However, at very low longitudinal speeds, there might be some infeasible maneuvers, like a vehicle only moving laterally with zero longitudinal speed. To address this issue, this sub-objective suppresses such vehicle maneuvers by penalizing excessive rates of lateral versus longitudinal speeds via the following function:

$$f_i^c = \begin{cases} (\beta v_{x,i}(k) - |v_{y,i}(k)|)^2 & \text{if } |v_{y,i}(k)| > \beta v_{x,i}(k) \\ 0 & \text{otherwise} \end{cases} \quad (11)$$

where β has a small and positive value [20].

C. Problem Formulation

The objective function including all the sub-objectives is given in (12). In contrast to the de-centralized case [20], where a similar OCP is formulated and minimized for each individual vehicle independently, the goal here is to minimize a collective cost function that holds all the vehicles' costs as follows:

$$J = \sum_{k=0}^{K-1}\sum_{i=1}^{n}\Bigg(\frac{1}{2}b_1(a_{x,i}(k))^2 + \frac{1}{2}b_2(a_{y,i}(k))^2 + \frac{1}{2}b_3(v_{x,i}(k)-v^*_{x,i})^2 + \frac{1}{2}b_4(v_{y,i}(k)-v^*_{y,i})^2 + \frac{1}{2}b_5 f_i^c + b_6\sum_{j=i+1}^{n} c_{ij}(\boldsymbol{x}_i,\boldsymbol{x}_j)\Bigg) \quad (12)$$

where b_1 to b_6 are weighting factors for each one of the sub-objectives to be chosen appropriately; and K is the time horizon. The accelerations $a_{x,i}$ and $a_{y,i}$ are functions of the new control variables u_x and u_y as explained in (7).

III. NUMERICAL SOLUTION

The general form of the considered OCP is:

$$J = \sum_{k=0}^{K-1}\Phi[\boldsymbol{x}(k),\boldsymbol{u}(k)] \quad (13)$$

$$\boldsymbol{x}(k+1) = \boldsymbol{f}[\boldsymbol{x}(k),\boldsymbol{u}(k)] \quad (14)$$

$$\boldsymbol{u}^{\min} \le \boldsymbol{u}(k) \le \boldsymbol{u}^{\max} \quad (15)$$

where $\boldsymbol{u}^{\min}$ and $\boldsymbol{u}^{\max}$ are constant lower and upper bounds on controls, respectively. The Hamiltonian function of this OCP reads:

$$H[\boldsymbol{x}(k),\boldsymbol{u}(k),\boldsymbol{\lambda}(k+1)] = \boldsymbol{\lambda}(k+1)^T\boldsymbol{f}[\boldsymbol{x}(k),\boldsymbol{u}(k)] + \Phi[\boldsymbol{x}(k),\boldsymbol{u}(k)] \quad (16)$$

where $\lambda(k)$ are the co-states, associated with the state equations. The necessary conditions for a local minimum are given below. The state equation is:

$$\boldsymbol{x}(k+1) = \frac{\partial H}{\partial \boldsymbol{\lambda}(k+1)} = \boldsymbol{f}[\boldsymbol{x}(k),\boldsymbol{u}(k)] \quad (17)$$

The control condition is as follows:

$$\frac{\partial H}{\partial u_i(k)} = \begin{cases} <0 & \text{if} \quad u_i(k) = u_i^{\max} \\ =0 & \text{if} \quad u_i^{\min} \le u_i(k) \le u_i^{\max} \\ >0 & \text{else} \quad u_i(k) = u_i^{\min} \end{cases} \quad (18)$$

Taken for all control variables $u_i(k)$. The co-state equation is:

$$\boldsymbol{\lambda}(k) = \frac{\partial H}{\partial \boldsymbol{x}(k)} \quad (19)$$

and the boundary conditions are given by:

$$\boldsymbol{x}(0) = \boldsymbol{x}_0, \qquad \boldsymbol{\lambda}(K) = 0 \quad (20)$$

An efficient FDA is employed to solve this OCP numerically [20], [22]. The algorithm eliminates implicitly the state equations and uses the necessary conditions of optimality to solve the OCP in the strongly reduced space of the control variables, i.e. in an mK-dimensional space, where m is the number of control variables. The goal is to reach a control vector $\boldsymbol{u}(k)$, $k = 0,...,K-1$, that corresponds to a local minimum of the cost function, while satisfying the state equations and all constraints. To this end, FDA exploits the fact that $\boldsymbol{g}(k) = \partial H/\partial \boldsymbol{u}(k) = [\partial \boldsymbol{f}/\partial \boldsymbol{u}(k)]^T\boldsymbol{\lambda}(k+1) + \partial\Phi/\partial\boldsymbol{u}(k)$ equals the reduced gradient in the mK-dimensional space of controls, if the states and co-states involved in the partial derivative satisfy the state and co-state equations. The control variables should not violate the constant boundary constraints; therefore, the saturation vector function is defined with the components:

$$\text{sat}_i(\boldsymbol{u}(k)) = \begin{cases} u_i^{\max} & \text{if} \quad u_i(k) > u_i^{\max} \\ u_i(k) & \text{if} \quad u_i^{\min} \le u_i(k) \le u_i^{\max} \\ u_i^{\min} & \text{else} \quad u_i(k) < u_i^{\min} \end{cases} \quad (21)$$

Also, the projected gradient $\boldsymbol{\gamma}$, to account for active constraints is defined as:

$$\gamma_i(k) = \begin{cases} 0 & \text{if} \quad u_i(k) = u_i^{\min} \text{ and } g_i(k) > 0 \\ 0 & \text{if} \quad u_i(k) = u_i^{\max} \text{ and } g_i(k) < 0 \\ g_i(k) & \text{else} \end{cases} \quad (22)$$

FDA is an iterative algorithm that starts with a feasible initial guess of the control trajectories. At each iteration, using reduced gradient information, an appropriate step in the mK-dimensional control space is taken in an attempt to improve control trajectories. In this paper, the potentially improved control trajectory is derived by using Resilient backpropagation (RPROP) [22], [23]. The RPROP method computes the necessary changes for the control variables, $\Delta u_i^{(l)}(k)$, based only on the signs of the gradient components as follows:

$$\Delta u_i^{(l)}(k) = \begin{cases} -\text{sign}(g_i^{(l)}(k)) & \text{if } g_i^{(l-1)}(k)g_i^{(l)}(k) > 0 \\ \eta^+\Delta u_i^{(l-1)}(k) & \\ -\text{sign}(g_i^{(l)}(k)) & \text{if } g_i^{(l-1)}(k)g_i^{(l)}(k) < 0 \\ \eta^-\Delta u_i^{(l-1)}(k) & \\ \Delta u_i^{(l-1)}(k) & \text{otherwise} \end{cases} \quad (23)$$

where $0 < \eta^- < 1 < \eta^+$. In words, the method treats each control $u_i(k)$ separately and takes a step in the negative direction of the corresponding gradient $g_i(k)$. If the gradient changed sign since the last iteration, then a component minimum has been just overrun, hence the step size is reduced via η^- while stepping back. If the gradient has the same sign as in the last iteration, then the step is increased via η^+ to advance faster towards the component minimum. The updated control trajectory is fed to the next iteration, until a sufficiently low projected-gradient norm is obtained. The algorithmic steps of FDA are presented below:

1:	Receive initial states
2:	Guess a feasible initial control trajectory $\boldsymbol{u}^{(0)}(k)$ for $k = 0,...,K-1$

3:	Compute states $\boldsymbol{x}^{(0)}(k)$ for $k=0,...,K-1$ from (17) with initial value (20)
4:	Compute co-states $\boldsymbol{\lambda}^{(0)}(k)$ for $k=0,...,K-1$ from (19), starting with (20)
5:	Compute $\boldsymbol{g}^{(0)}(k)$
6:	Set iteration index $l=0$
7:	**while** $l <$ max-iterations
8:	Compute $\boldsymbol{u}^{(l+1)}(k)=\text{sat}[\boldsymbol{u}^{(l)}(k)+\Delta\boldsymbol{u}^{(l)}(k)]$ and $\boldsymbol{x}^{(l+1)}(k)$ for $k=0,...,K-1$ from (17) with initial value (20)
9:	Compute co-states $\boldsymbol{\lambda}^{(l+1)}(k)$ for $k=0,...,K-1$ from (19), starting with (20)
10:	Compute $\boldsymbol{g}^{(l+1)}(k)$
11:	Compute projected gradient $\boldsymbol{\gamma}^{(l+1)}(k)$
12:	**if** not converge
13:	Index increment $l=l+1$
14:	**continue**
15:	**else**
16:	**break**
17:	**end if**
18:	**end while**
19:	Generate optimal control input $\boldsymbol{u}(k)$ for $k=0,...,K-1$

FDA iterations can be stopped at any time, even before convergence, delivering a control trajectory that is feasible, i.e., satisfies all state equations and constraints, but may be sub-optimal. It should be noted that the OCP at hand is non-convex, hence the delivered minimum can be a local minimum. However, if this local minimum serves the purposes of the problem, as discussed in the next section, then the local minimum can be accepted.

IV. Preliminary Results

A. Scenario Setup

To demonstrate the efficiency of the proposed approach, two challenging scenarios are tested, each considering a group of 8 vehicles driving lane-free on a straight road. Every vehicle has its own longitudinal desired speed and zero lateral desired speed. At the initial state, the vehicles are positioned behind each other at around the center of the road (Figs. 2, 3), with inter-vehicle distances of 40 m, and in inverse order of their longitudinal desired speeds; therefore, vehicles need to overtake one another, via appropriate maneuvers, and reach their desired speeds. Thus, at the end of the time horizon, vehicles' longitudinal positions will be ordered according to their desired speeds, meaning that the fastest vehicle (with the highest desired speed value) should be the first vehicle of the group; the second-fast vehicle should be second in positioning order and so on; and the time horizons are taken sufficiently long to cover this re-ordering of longitudinal vehicle positions.

TABLE I. SCENARIO 1 CHARACTERISTICS

Vehicle No.	**1**	**2**	**3**	**4**	**5**	**6**	**7**	**8**
$x(0)$ in (m)	0	40	80	120	160	200	240	280
$y(0)$ in (m)	4.9	5.2	5.0	5.1	4.8	5.3	4.9	5.2
v_x^* in (m/s)	17	16	15	14	13	12	11	10
$v_x(0)$ in (m/s)	10	10	10	10	10	10	10	10

TABLE II. SCENARIO 2 CHARACTERISTICS

Obstacle No.	**1**	**2**	**3**
$x(0)$ in (m)	450	458	600
$y(0)$ in (m)	1.0	1.0	1.0

A lane-free straight road with 10.2 m width is considered for the tests. All the vehicles have same dimensions of 5 m length and 2 m width. The parameters used for the ellipsoid are $p_1=6$, $p_2=p_3=p_4=p_5=2$ in (8) and $\omega_1=0.6$ s, $\omega_2=0.5$ s, $\mu_x=\mu_y=1$, $\varepsilon_\omega=0.1$ in (10). β is set to 0.03 in (11); while the RPROP parameters in (23) are $\eta^+=1.2$ and $\eta^-=0.5$. In (12), the penalty weights are $\{b_1,b_2,b_3,b_4,b_5,b_6\}=\{0.1,0.1,0.01,0.1,0.1,3.0\}$ and the discrete time step is $T=0.25$ s. All longitudinal initial speeds are 10 m/s, and all lateral initial speeds are zero. The longitudinal desired speeds are given in Table 1, while the lateral desired speeds are zero. The constant longitudinal acceleration bounds are $A^{\max}=1.5\ \text{m/s}^2$ and $A^{\min}=-2\ \text{m/s}^2$. Two scenarios are investigated as follows.

It is interesting to note that, if the group of vehicles would be initially perfectly aligned (something that exists only in mathematics), i.e., if all vehicles would have the exact same initial lateral positions, this would lead to a local minimum whereby the vehicles remain at the same lateral position for the whole optimization time horizon, meaning that they would get trapped behind each other.

In Scenario 1, the road is empty in front of the 8 vehicles (Fig. 2). In Scenario 2, there are three vehicles (see Fig. 3) in front, which are not optimized, but drive independently. Specifically, for these three vehicles, it is assumed that longitudinal and lateral speeds are constant during the whole optimization time horizon, i.e., they have zero accelerations.

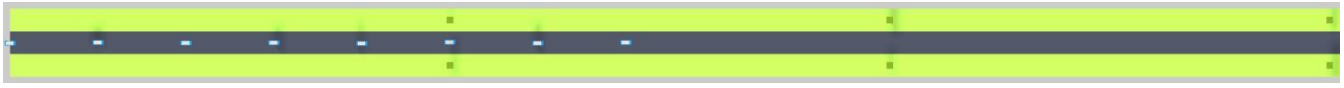

Figure 2. Scenario 1 vehicle arrangement

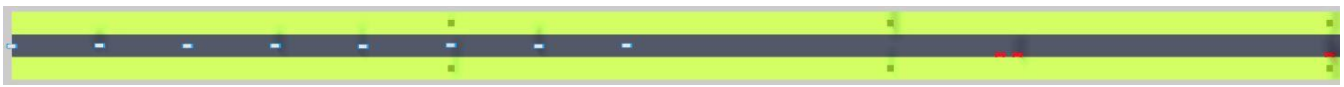

Figure 3. Scenario 2 vehicle arrangement

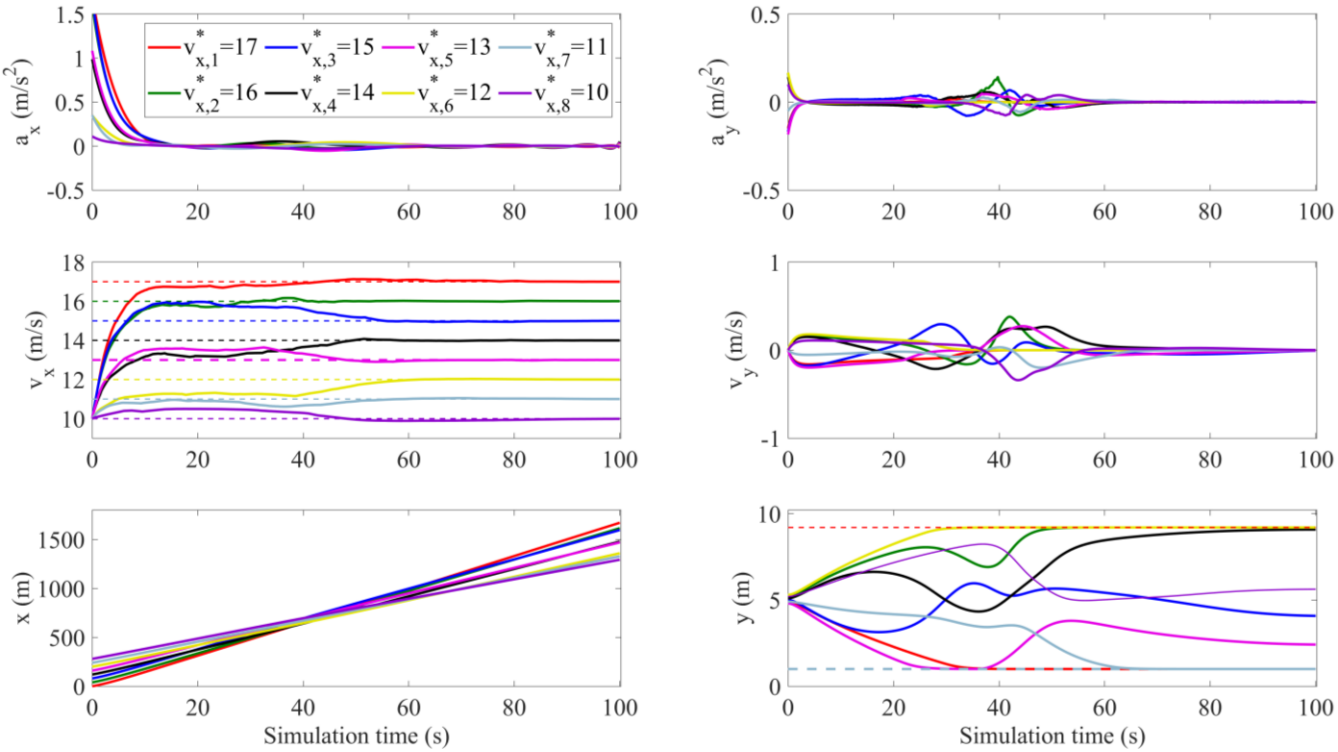

Figure 4. Optimal longitudinal and lateral trajectories for all 8 vehicles in Scenario 1

However, the three vehicles are accounted for in the collision avoidance term, i.e., they are considered as independent moving or standing obstacles to be avoided by the 8 vehicles of the group. Two of these obstacles are stopped at the road boundary, emulating an incident; while the third obstacle is moving with a constant speed of 10 m/s on the right road boundary. Initial positions of the obstacles are given in Table II. Finally, the optimization horizons are 100 s for Scenario 1 and 125 s for Scenario 2.

B. Results

Fig. 4 displays the longitudinal and lateral movements of all 8 vehicles of the group in Scenario 1. It can be seen that all the vehicles have successfully reached their desired speeds and taken their natural longitudinal positioning order within 100 s of time horizon ($K = 400$). FDA needed 5.58 s of CPU time to converge, coded in C and run on an Intel(R) Core TM i5-10500 CPU @ 3.10GHz with 8.0 GB installed RAM. It should be noted that the employed convergence test to reach the reported results was quite strict. It was found that, if the FDA iterations are stopped earlier, the obtained results are similarly good from an application point of view, while the computation time is reduced to around 1.5 s. As the longitudinal-position diagram in Fig. 4 indicates, the initial positioning of the vehicles is indeed utterly reversed at the end of the time horizon, e.g., the fastest vehicle that initially was the last vehicle of the group, is the first at the end of the time horizon, and also the rest of the vehicles are located according to their desired speeds. In Fig. 4, longitudinal accelerations are moderate in magnitude, which saves fuel consumption. It should be mentioned that the RPROP method has the tendency to deliver trajectories that are not fully smooth; therefore, the longitudinal accelerations delivered by FDA were smoothified for improved passenger convenience.

The reverse ordering of the vehicles required a plethora of appropriate vehicle maneuvers and multiple overtaking (involving combined lateral and longitudinal actions of all vehicles) that result spontaneously from the optimization procedure. Despite this vivid re-ordering with partly strong lateral positioning changes (Fig. 4), the lateral accelerations and speeds are low in magnitude and smooth, leading to flexible and elegant lateral maneuvers that serve the goal. Needless to say that no collisions occur, as the optimization avoids the high cost that would result from the collision avoidance term, whose value in the results is close to zero. Furthermore, it is worth observing that some vehicles are nudged towards a lateral road boundary, in order to make room for faster vehicles that are moving behind them to overtake. Some of them may continue driving exactly on the road boundary, as they have no reason to change course. These movements demonstrate and verify the role of the lateral constraints (5), (6).

In Fig. 5, trajectories for Scenario 2 are presented. The same group of vehicles now faces three obstacles on its way, which further complicates the required maneuvers and calls for a longer time horizon of 125 s ($K = 500$) to complete the longitudinal position reversing. This took 26.46 s of CPU time for FDA to converge, but again this time can be sensibly reduced if FDA iterations are stopped earlier without really affecting the outcome from an application viewpoint.

This scenario is more challenging than the previous one, as each vehicle must deal with obstacles as well as with other vehicles of the group. Therefore, the amount of necessary maneuvers increases, affecting both longitudinal and lateral movements, but all control and state trajectories of all vehicles remain very moderate and smooth.

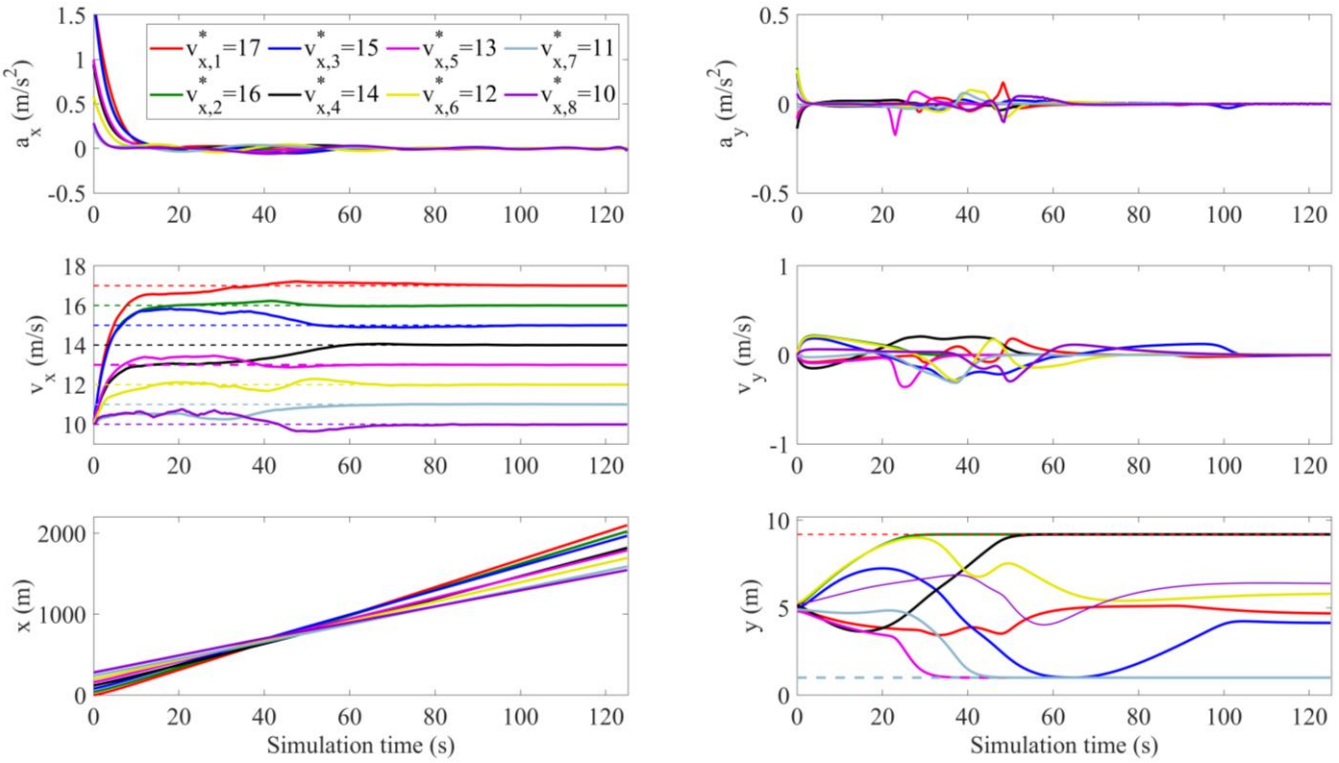

Figure 5. Optimal longitudinal and lateral trajectories for 8 control vehicles in Scenario 2

As an example of intelligent maneuvering emerging spontaneously from the optimization procedure, consider vehicle #5 around the time $t = 25$ s, when this vehicle, driving at a longitudinal speed close to its desired speed $v^*_{x,5} = 13$ m/s, is overtaking the stationary obstacles that are located at the right road boundary. Soon after overtaking the obstacles, the vehicle moves towards the right road boundary to make space for faster vehicles behind to pass. This is visible in the vehicle's lateral positioning, but also in the small negative peak in its lateral acceleration that is clearly visible in Fig. 5.

Similarly, to Scenario 1, at the end of this scenario, vehicles manage to successfully reach their respective desired longitudinal speeds and to reverse their longitudinal position ordering, while at the same time overtaking the obstacles without any collision. Note that, also in this scenario, longitudinal acceleration trajectories were smoothified to provide more comfort for the passengers.

Corresponding videos, demonstrating more lively the performance of the proposed approach for both scenarios, are available in (https://bit.ly/3OS3rZl).

V. Conclusions

An optimal joint path-planning approach is developed and applied to control simultaneously a number of vehicles to optimize their trajectories in a coordinated way. In the proposed approach, an objective function is formulated for a group of vehicles, taking into account efficiency, safety and passenger comfort. This optimal control problem is solved numerically with efficient Nonlinear Programming techniques in the reduced controls space and using the resilient backpropagation method to update control trajectories at each iteration. The procedure converges to a local minimum that was always found to be satisfactory from an application point of view. The approach is applied to a group of connected and automated vehicles in a lane-free traffic environment with vehicle nudging. It is demonstrated that vehicles move efficiently and safely in a coordinated way, each one of them achieving its desired speed value, relative position and maintaining passenger convenience, while fully respecting the road boundaries. This is achieved via smooth and intelligent maneuvering that emerges spontaneously from the optimal control problem solution. Computation times to solve the optimal control problem are reasonable and can be further lowered.

Current work is focused on:

- Comparison of the centralized and decentralized path-planning to evaluate the efficiency benefits offered by the proposed coordinated approach.
- Application in more complicated scenarios (introducing on-ramps, off-ramps and higher traffic densities).
- Implementation of the proposed approach in an MPC framework.

In a nutshell, the paper describes the development of a methodological and computational tool for intelligent control of a group of vehicles in a coordinated way in lane-free traffic. There are multiple potential applications of this tool. In particular, while [20] considered independent MPC-based driving for individual vehicles, the present tool, employed in an MPC mode, allows for a variety of different entities to be considered in lane-free traffic, each of which is being controlled in an independent way. Such entities may comprise individual vehicles, groups of vehicles, vehicle platoons in different formations (e.g., vehicle flocks, 2-D snake-like platoons) and more.

REFERENCES

[1] C. Diakaki, M. Papageorgiou, I. Papamichail, and I. Nikolos, "Overview and analysis of vehicle automation and communication systems from a motorway traffic management perspective," *Transportation Research Part A: Policy and Practice,* vol. 75, pp. 147-165, 2015.

[2] U. Montanaro, S. Dixit, S. Fallah, M. Dianati, A. Stevens, D. Oxtoby, and A. Mouzakitis, "Towards connected autonomous driving: review of use-cases," *Vehicles System Dynamics*, vol. 57, no. 6, pp. 779-814, 2019.

[3] K. Sjoberg, P. Andres, T. Buburuzan, and A. Brakemeier, "Cooperative intelligent transport systems in Europe: Current deployment status and outlook," *IEEE Vehicular Technology Magazine*, vol. 12, no. 2, pp. 89-97, 2017.

[4] M. Papageorgiou, K.S. Mountakis, I. Karafyllis, I. Papamichail, and Y. Wang, "Lane-free artificial-fluid concept for vehicular traffic," *Proceedings of the IEEE*, vol. 109, no. 2, pp. 114-121, 2021.

[5] J. Guanetti, Y. Kim, and F. Borrelli, "Control of connected and automated vehicles: State of the art and future challenges," *Annual reviews in control*, vol. 45, pp. 18-40, 2018.

[6] L. Claussmann, M. Revilloud, D. Gruyer, and S. Glaser, "A review of motion planning for highway autonomous driving," *IEEE Transactions on Intelligent Transportation Systems*, vol. 21, no. 5, pp. 1826-1848, 2019.

[7] Y. Wang, X. Li, and H. Yao, "Review of trajectory optimization for connected automated vehicles," *IET Intelligent Transportation Systems*, vol. 13, no. 4, pp. 580–586, 2018.

[8] M.A.S. Kamal, S. Taguchi, and T. Yoshimura, "Efficient driving on multilane roads under a connected vehicle environment," *IEEE Transactions on Intelligent Transportation Systems*, vol. 17, no. 9, pp. 2541-2551, 2016.

[9] P. Typaldos, M. Papageorgiou, and I. Papamichail, "Optimization-based path-planning for connected and non-connected automated vehicles," *Transportation Research Part C: Emerging Technologies*, vol. 134, Article 103487, 2022.

[10] S. Dixit, U. Montanaro, M. Dianati, D. Oxtoby, T. Mizutani, A. Mouzakitis, and S. Fallah, "Trajectory planning for autonomous high-speed overtaking in structured environments using robust MPC," *IEEE Transactions on Intelligent Transportation Systems,* vol. 21, no. 6, pp. 2310-2323, 2019.

[11] J. Rios-Torres and A.A. Malikopoulos, "A survey on the coordination of connected and automated vehicles at intersections and merging at highway on-ramps," *IEEE Transactions on Intelligent Transportation Systems*, vol. 18, no. 5, pp. 1066-1077, 2016.

[12] T. Li, J. Wu, C.-Y. Chan, M. Liu, C. Zhu, W. Lu, and K. Hu, "A cooperative lane change model for connected and automated vehicles," *IEEE Access*, vol. 8, no. 2, pp. 54940-54951, 2020.

[13] C. Burger and M. Lauer, "Cooperative multiple vehicle trajectory planning using MIQP," *21st IEEE International Conference on Intelligent Transportation Systems (ITSC)*, Maui, Hawaii, USA, November 4-7, pp. 602-607, 2018.

[14] Y. Sakaguchi, A.S.M. Bakibillah, Md.A.S. Kamal, and K. Yamada, "A cyber-physical framework for optimal coordination of connected and automated vehicles on multi-lane freeways," *MDPI Sensors*, vol. 23, no. 2, 611, 2023.

[15] R. Levy and J. Haddad, "Cooperative path and trajectory planning for autonomous vehicles on roads without lanes: A laboratory experimental demonstration," *Transportation Research Part C: Emerging Technologies*, vol. 144, Article 103813, 2022.

[16] A. Madridano, A. Al-Kaff, D. Martín, and A. de la Escalera "Trajectory planning for multi-robot systems: Methods and applications," *Expert Systems with Applications,* vol. 173, Article 114660, 2021.

[17] A. Israr, Z.A. Ali, E.H. Alkhammash, and J.J. Jussila, "Optimization methods applied to motion planning of unmanned aerial vehicles: A review," *MDPI Drones*, vol. 6, no. 5, 126, 2022.

[18] S. Shao, Y. Peng, C. He, and Y. Du, "Efficient path planning for UAV formation via comprehensively improved particle swarm optimization," *ISA Transactions*, vol. 97, pp.415-430, 2020.

[19] Z. A. Ali, H. Zhangang, and W.B. Hang, "Cooperative path planning of multiple UAVs by using max–min ant colony optimization along with Cauchy Mutant operator," *Fluctuation and Noise Letters*, vol. 20, no. 1, 2150002, 2020.

[20] V. K. Yanumula, P. Typaldos, D. Troullinos, M. Malekzadeh, I. Papamichail, and M. Papageorgiou, "Optimal path planning for connected and automated vehicles in lane-free traffic with vehicle nudging," *IEEE Transactions on Intelligent Vehicles*, vol. 8, no. 3, pp. 2385-2399, 2023.

[21] P. Typaldos, I. Papamichail, and M. Papageorgiou, "Minimization of fuel consumption for vehicle trajectories," *IEEE Transactions on Intelligent Transportation Systems*, vol. 21, no. 4, pp. 1716-1727, 2020.

[22] M. Papageorgiou, M. Marinaki, P. Typaldos, and K. Makantasis, "A feasible direction algorithm for the numerical solution of optimal control problems-extended version," *Chania, Greece: Technical University of Crete, Dynamics Systems and Simulations Laboratory*, no. 2016-26, 2016.

[23] A. Kotsialos, "Nonlinear optimization using directional step lengths based on RPROP," *Optimization Letters*, vol. 8, pp. 1401-1415, 2014.